Drop-on-demand printing of complex liquids

Neil F. Morrison and Oliver G. Harlen; Department of Applied Mathematics; University of Leeds, Leeds, LS2 9JT, U.K.

Abstract

We investigate the influence of fluid properties on jet breakup in the context of drop-on-demand inkjet printing. In drop-on-demand printing, each drop remains connected to the printhead by a ligament which thins while the drop is in flight. Upon pinch-off the severed ligament may recoil into the leading drop, or (more commonly for high-speed printing) the ligament may fragment into 'satellite drops' which reduce printing resolution. A key goal of inkjet research is to prevent or impede the creation of satellite drops without compromizing on printing speed. Viscoelastic and shear-thinning fluids may, in rather different ways, exhibit enhanced resistance to fragmentation in jetting flows compared to Newtonian fluids of similar viscosity. In this work we seek to explore and exploit this behaviour with the overall aim of increasing the proportion of ejected ink contained within the main drop when printing at a prescribed drop velocity. Using Lagrangian finite-element simulations under realistic industrial inkjet conditions, we consider a non-Newtonian fluid model which incorporates both viscoelastic and thixotropic effects simultaneously. We discuss how appropriate values of the rheological parameters may be chosen so as to optimize the fluid's transient viscosity at different key stages of a drop-on-demand flow cycle, and how our results may be beneficial to industrial and commercial applications of inkjet technology.

Introduction

Among the major challenges in contemporary inkjet research are the enhancements of the speed, resolution, and material diversity of the printing process in order to broaden the range of industrial and commercial applications and improve existing technology. These challenges may be addressed in a number of ways depending on the extent to which each constituent part of the process may be modified, for example, by redesigning the internal structure of the printhead or changing the actuation waveform that drives the jetting, or by adjusting the fundamental fluid properties of the ink (chiefly its viscosity and surface tension). An extension of the latter approach involves the exploitation of non-Newtonian fluid phenomena, and in recent times this has led to the development of several new applications of inkjet technology [1] [2]. Viscoelastic effects may influence jetting behaviour profoundly [3] [4], as may the presence of a particulate phase [5].

Due to the various ingredients necessary to provide the required levels of performance and chemical stability, the majority of fluids used in real inkjet applications are, in essence, colloidal suspensions and consequently they may exhibit some degree of non-Newtonian behaviour when subjected to rheological characterization [6]. The local variation of viscosity in such a fluid can influence the breakup dynamics of a particle-laden jet compared to those of Newtonian jets [7], and may therefore determine whether the fluid is suitable for a particular application. Conversely, the capacity to impose explicit control upon the breakup behaviour, by making appropriate modifications to the rheological properties of the ink, is an important versatility requirement of industrial and commercial printing technologies [8]. A detailed understanding of the effects of rheology on breakup is thus an ongoing ambition of inkjet research.

In a drop-on-demand (DOD) inkjet printer each individual drop is formed by the ejection of a finite ligament of ink from one of an array of nozzles located directly above the target area for deposition. This ligament subsequently either disintegrates into a main drop and a series of smaller 'satellite' drops, or, preferably, contracts to form a single drop, before impacting on the target substrate. The fate of the ligament depends mainly on the speed of printing and on the ink viscosity and surface tension (i.e. the Reynolds, Weber, and Ohnesorge numbers of the flow) which control its rate of capillary thinning [9]. In almost all applications the production of satellite drops in significant number or volume is considered highly undesirable due to reduced resolution in the printed output.

Historically there have been few studies of the printing of non-Newtonian fluids, although the subject has undergone substantial development in recent years as the complexity of the fluid dynamics and the rich potential for novel applications have fueled research in this area [1] [2]. Experimental studies of the DOD printing of polymer solutions have revealed a diverse family of viscoelastic jet behaviour depending on the concentration and molecular weight of the polymer. The observations of Bazilevskiy et al. [10], Shore and Harrison [11], Hoath et al. [12], Xu et al [13], and Yan et al. [14] have shown consistently the same phenomena for a variety of polymers and over a range of operating conditions; these phenomena have been reproduced in simulations by the present authors, both qualitatively [15] and quantitatively [16]. Even small amounts of polymer can cause severely different breakup dynamics compared to Newtonian printing, influencing both in-flight fragmentation and detachment from the nozzle, and significant concentrations can also impede jettability due to high elasticity in the ligament.

More generally the introduction of a polymeric component, even at a low concentration, can significantly alter the dynamics of free-surface breakup [17]. The profound effects of elasticity are sufficiently robust that data extracted from measurements of capillary thinning flows have been used to provide fluid rheometry [18], and to establish the validity of computational schemes for viscoelastic flow [19]. Elasticity accelerates the initial growth of the capillary instability but prolongs the overall lifespan of a thinning fluid filament, delaying its eventual breakup, as was shown in an early study by Goldin et al. [3]. Unlike the Newtonian case, the radius of a thinning filament of polymeric fluid decreases at an exponential rate (based on the relaxation timescale of the polymer) while the molecules are undergoing elongation [20], before deviating rapidly towards finite-time breakup as the molecules become fully extended [21]. The finer details of the dynamics vary

to some degree with the choice of constitutive model [22]. Depending on its initial aspect ratio, a viscoelastic filament may also develop the self-similar pattern described as 'beads on a string' or 'blistering' [23].

Shear-thinning fluid models have received somewhat less attention, but have also been shown to exhibit markedly different behaviour in filament stretching flows [24] and jet breakup [25] compared to the purely Newtonian case. Doshi et al. [26] performed a thorough analysis of capillary thinning rates for a Carreau fluid [27] (and a power-law fluid as a limiting case), which complemented contemporary work by Renardy [28] [29]. Drop formation has been addressed, as in computational work by Yıldırım and Basaran [30] who studied the influence of both shear-thinning and shear-thickening rheology on dripping over a range of flow rates, finding a rich family of regular and irregular patterns; parameters conducive to the potential suppression of satellite drops were also discussed. Experiments on the formation of pendant drops of particle suspensions have also suggested the reduction of satellites [5] [7] [31]. A recent experimental survey by Clasen et al. [32] concerning the ejection of a variety of complex fluids through millimetre-sized needles has provided a valuable summary of non-Newtonian effects, including shear-thinning. In a study more specific to high-speed printing, the present authors have shown in simulations of Carreau fluids that shear-thinning behaviour may reduce both the number and sizes of satellites when printing at a prescribed main drop velocity [16], and recent experiments by Hoath et al. [33] have corroborated these overall conclusions.

In this work we consider the influence of non-Newtonian rheology on ligament breakup in DOD simulations; we use a fluid model with both viscoelastic and shear-thinning attributes, and we explore its parameter space with the aim of increasing the proportion of ejected ink contained within the main drop when printing at fixed speed.

Numerical method and boundary conditions

The simulations use an axisymmetric Lagrangian finite-element method first developed for the study of creeping flow of dilute polymer solutions [34]. The method has since been extended to inertial flows and has been applied to inkjet printing of Newtonian and complex fluids [35] [15] [16]; details of the computational methods may be found in these references. The shape of the nozzle used in the simulations is identical to that in references [15] and [16], based on a Xaar 126 printhead with nozzle radius $R = 25\,\mu\text{m}$. At the nozzle inlet a time-dependent velocity boundary condition is imposed in the form of a 'pull/push/pull' drive waveform of $\approx 30\,\mu\text{s}$ duration; this waveform is amplified in each simulation in order to attain a prescribed drop speed $U = 6\,\text{m}\,\text{s}^{-1}$ for all fluids modelled. Consequently the total volume of ejected ink is not necessarily constant.

We assume that the jet is axisymmetric, so that it may be fully described by a cylindrical coordinate system $\{r,\theta,z\}$ with all flow variables independent of θ. The origin is taken as the centre of the nozzle outlet, and the fluid is initially at rest. The boundary conditions at the free surface are those of zero shear stress and the pressure jump due to surface curvature,

$$\hat{\mathbf{n}}\cdot\boldsymbol{\sigma}\cdot\hat{\mathbf{t}} = 0\,, \qquad \left[\boldsymbol{\sigma}\cdot\hat{\mathbf{n}}\right]_{\text{air}}^{\text{jet}} = -\frac{1}{\text{We}}\left(\frac{1}{R_1}+\frac{1}{R_2}\right)\hat{\mathbf{n}}\,, \qquad (1)$$

where $\boldsymbol{\sigma}$ is the dimensionless stress tensor, $\hat{\mathbf{n}}$ is the unit outward normal to the interface, $\hat{\mathbf{t}}$ is the unit tangent in the rz-plane, and R_1 and R_2 are the principal radii of curvature. External air pressure is neglected. Symmetry conditions on the z-axis are $u_r = 0$ and $\sigma_{rz} = 0$, and conditions of no-slip are applied at the rigid interior printhead boundaries. The contact line between the free surface and the printhead is held pinned at the nozzle edge throughout.

The location of the free surface at each time-step is determined implicitly via a kinematic condition. In the simulations this is realized automatically, since the mesh is Lagrangian and the mesh nodes are advected with the local fluid velocity. Drag due to air resistance is neglected, as are temperature variations.

Fluid model and governing equations

The governing equations are the conservation of momentum and mass for an incompressible dilute polymer solution

$$\rho\frac{\text{D}\mathbf{u}}{\text{D}t} = \nabla\cdot\boldsymbol{\sigma}\,, \qquad \nabla\cdot\mathbf{u} = 0\,, \qquad (2)$$

where ρ is the fluid density, t and $\mathbf{u}$ are the time and fluid velocity respectively, and $\boldsymbol{\sigma}$ is the stress tensor which may be expressed as

$$\boldsymbol{\sigma} = -p\mathbf{I} + 2\mu_S\mathbf{E} + \frac{\mu_P}{\tau}(\mathbf{A}-\mathbf{I})\,, \qquad (3)$$

where p is pressure, μ_S is the solvent viscosity, μ_P is the polymeric contribution to the viscosity, τ is the relaxation time, $\mathbf{E} = \frac{1}{2}\left(\nabla\mathbf{u} + (\nabla\mathbf{u})^T\right)$ is the rate of strain tensor, and $\mathbf{A}$ is the polymeric structure tensor.

In this work we use the single mode Giesekus fluid model [36] which incorporates both viscoelastic and shear-thinning behaviour. For this model the structure tensor satisfies the following evolution equation:

$$\overset{\triangledown}{\mathbf{A}} \equiv \frac{\text{D}\mathbf{A}}{\text{D}t} - \mathbf{A}\cdot\nabla\mathbf{u} - (\nabla\mathbf{u})^T\cdot\mathbf{A} = -\frac{1}{\tau}(\mathbf{A}-\mathbf{I}) - \frac{\alpha}{\tau}(\mathbf{A}-\mathbf{I})^2\,, \qquad (4)$$

where α is a dimensionless parameter (sometimes called the mobility factor [37]) which controls the size of the non-linear term. When α is zero the Giesekus model reduces to the Oldroyd-B model, and when α is small there is an analogy with the FENE-CR model with extensibility $L \sim \alpha^{-1/2}$.

For fixed solvent viscosity and density, the range of non-Newtonian behaviour which may be modelled is controlled by three dimensionless parameters: (i) the 'concentration' $c = \mu_P/\mu_S$, (ii) the Weissenberg number $\text{Wi} = \tau/T$, which measures the relaxation time τ against a characteristic flow timescale $T = R/U$, and (iii) the mobility factor α mentioned above. These are in addition to the usual 'Newtonian' dimensionless quantities [38]: the Reynolds number $\text{Re} = \rho UR/\mu_S(1+c)$, the Weber number $\text{We} = \rho U^2R/\gamma$ (where γ is the surface tension), and the Ohnesorge number $\text{Oh} = \mu_S(1+c)/\sqrt{\rho\gamma R} = \sqrt{\text{We}}/\text{Re}$. Gravity is negligible on the lengthscales considered in this study. Throughout this work we keep ρ, μ_S, and γ constant, with $\text{We} \approx 14$, and we vary c (hence Re and Oh); typical values are $\text{Re} \approx 42$ and $\text{Oh} \approx 0.1$. For flows involving jet breakup it is common to define a capillary time $t_c = \sqrt{\rho R^3/\gamma} = T\sqrt{\text{We}}$ as the relevant timescale for inertio-capillary thinning [23].

Rheology and implications

In order to choose appropriate values of the parameters in the Giesekus fluid model, we consider how the transient viscosity of the fluid should vary during the three key phases of a drop-on-demand cycle. Firstly there is high shear during the 'push' stage of the driving waveform as fluid is ejected rapidly through the nozzle; in this phase the viscosity should be low for ease of ejection without excessive amplification (i.e. voltage). Secondly there is extension during the 'pull' stage of the driving which draws out a ligament behind the leading drop; the viscosity should remain quite low in this phase to allow prompt detachment of the ligament from the printhead, but not so low that the capillary instability develops fully along the ligament while it is still attached. Thirdly there is the thinning of the detached ligament, during which phase the viscosity should be high in order to delay breakup and maximize the proportion of ink which ultimately ends up within the main drop. We therefore wish to find values for the non-Newtonian parameters to optimize the fluid properties in each of these key phases.

One means of doing this without solving the full inverse problem is to compare the viscosity response functions for three standard rheometric flows: steady shear at rate $\dot{\gamma}$, steady extension at rate $\dot{\varepsilon}$, and small-amplitude oscillatory shear at frequency ω. The corresponding rheometric response functions[1] are the shear viscosity $\eta(\dot{\gamma})$, the extensional viscosity $\bar{\eta}(\dot{\varepsilon})$, and the complex viscosity magnitude $|\eta^*(\omega)|$; analytical expressions of these functions exist for the Giesekus fluid [37]. To plot the functions on common axes we define a Deborah number (De) equal to $\tau\dot{\gamma}$ for shear, $\tau\dot{\varepsilon}\sqrt{3}$ for extension, and $\tau\omega$ for oscillatory flow.

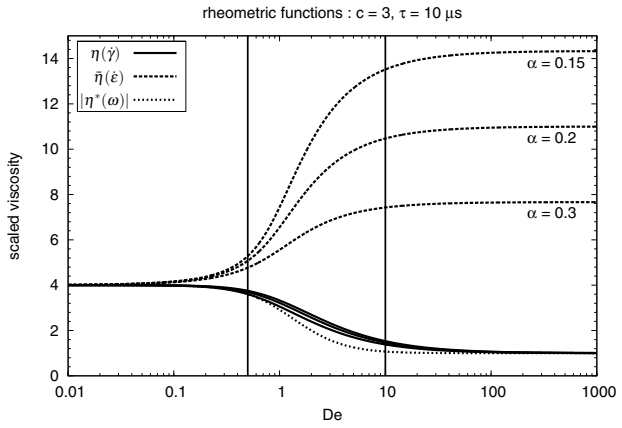

Figure 1. *The dependence of the rheometric functions on α.*

In Fig. 1 the rheometric functions are shown for three values of α, with the other parameters fixed: $c = 3$ and $\tau = 10\,\mu s$ (Wi = 2.4). For ease of comparison, η and $|\eta^*|$ are scaled by μ_S, and $\bar{\eta}$ by $3\mu_S$, to have a common intercept of $1 + c$ as De $\to 0$ (the zero shear rate limit). The corresponding asymptotes as De $\to \infty$ are 1 and $1 + 2c/3\alpha$. It is clear that the increase in extensional viscosity $\bar{\eta}$ is strongly dependent on α whereas the shear viscosity η is affected only modestly: the latter falls smoothly between its two asymptotes and in this sense c determines the magnitude of the shear-thinning transition for the cases shown. It should be noted that $|\eta^*|$ is actually independent of α [37]. The two vertical lines in Fig. 1 illustrate the estimated range of deformation rates most relevant to the key DOD flow phases discussed above, and thus we favour values of the viscoelastic parameters which yield significant transitions within this range. Because the rheometric functions depend on τ (hence Wi) only through the product De, the effect of varying τ is simply to shift these vertical lines horizontally: a value of around 10 μs gives optimal alignment of the viscosity transitions within the relevant range of Deborah number.

The combined influences of c and α on the magnitude of these viscosity transitions are illustrated in Figs 2 and 3 which show heat-maps and contours of the drop in shear viscosity η and the rise in extensional viscosity $\bar{\eta}$, respectively, between De = 0.5 and De = 10, i.e. between the two vertical lines plotted in Fig. 1. In simplistic terms one would like to choose c large enough to see substantial shear-thinning, and α large enough so that extension does not dominate. However it should be emphasized that the rheometric functions are defined for *steady* flows and should therefore be used only as a rough guide to how the fluid may respond to transient flow on the short timescales involved in DOD printing.

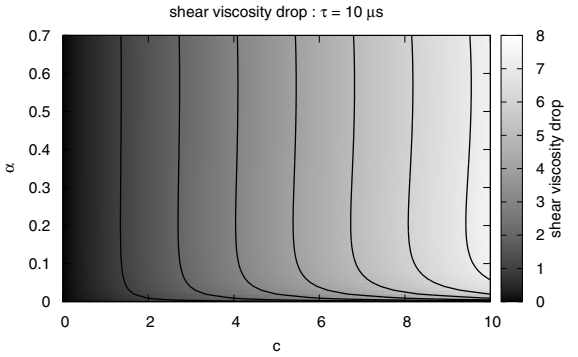

Figure 2. *The variation of the drop in scaled shear viscosity (η/μ_S).*

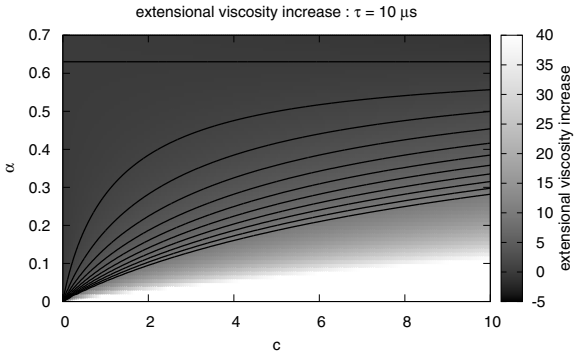

Figure 3. *The variation of the rise in scaled extensional viscosity $(\bar{\eta}/3\mu_S)$.*

Another consideration to be borne in mind when choosing parameter values is the empirical Cox-Merz rule [39], which is that η and $|\eta^*|$ have been found to be roughly equivalent as functions of Deborah number for a wide class of physical polymeric fluids; as illustrated in Fig. 1, the Giesekus fluid model follows this rule. The rheometric functions for the Giesekus model may be compared to those of other models studied previously; we note that for a generalized Newtonian fluid [16], η/μ_S and $\bar{\eta}/3\mu_S$ are identical functions of deformation rate $\dot{\gamma} = \dot{\varepsilon}\sqrt{3}$ (i.e. a Carreau fluid is also extension-thinning, as well as shear-thinning).

[1] Discussion of the first and second normal stress difference functions has been omitted for brevity.

Results

Free-surface shapes of the ejected ligament are plotted in Fig. 4 for several values of concentration, with the other parameters held constant. Each curve corresponds to time $t = 50\,\mu\text{s} = 12T$ during the flow, i.e. after the driving waveform has ended but before detachment. The radial and axial coordinates (r, z) are scaled by nozzle radius $R = 25\,\mu\text{m}$. There is clear enhancement of the development of the instability along the ligament surface with increasing concentration, as well as a growth of the leading drop radius due to the greater drive amplitude required to maintain an ultimate drop speed of $U = 6\,\text{m/s}$; similarly the meniscus is drawn back further inside the printhead ($z < 0$) at larger c.

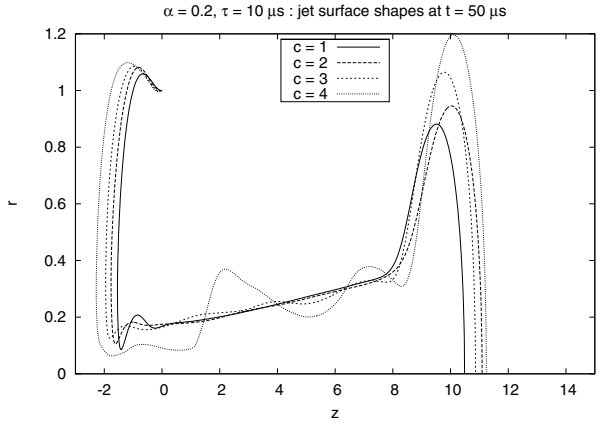

Figure 4. *Variation of ligament shapes with concentration; the direction of printing is left to right, with the nozzle plate at $z = 0$.*

Analogous plots for cases with varying α are shown in Fig. 5. The same trends of enhanced surface development and greater drop radius are found with increasing elasticity (decreasing α). These findings agree qualitatively with previous results on viscoelastic printing [15]. In addition the instantaneous length of the ligament increases at smaller α because the greater extensional resistance slows the leading drop while it remains attached to the printhead; since the ultimate detached drop speed is fixed, the drop speed at the instant shown is therefore faster when α is small.

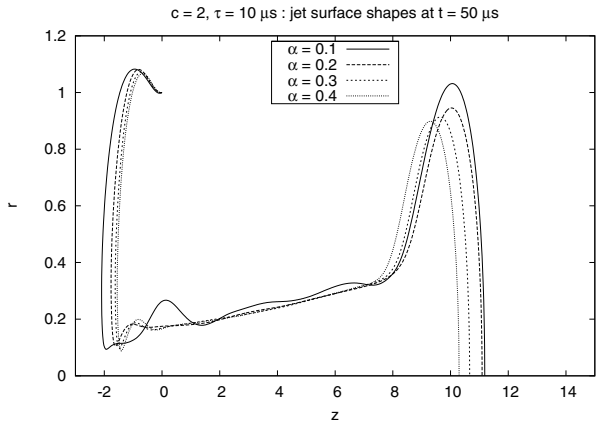

Figure 5. *Variation of ligament shapes with α.*

The drive amplification necessary to attain the specified main drop speed U for each choice of parameters was found by iteration; the required amplitude may be thought of as a measure of resistance to ejection. The variation of this amplitude with c and α (for fixed Wi = 2.4) is shown in Fig. 6, with values scaled relative to the case $c = 0$ (i.e. the Newtonian solvent has a drive amplitude of 1). Dependence on c is roughly linear for each set of fixed α, and dependence on α is approximately reciprocal for fixed c. Hence when plotted against the quotient c/α the amplitude data show reasonable collapse towards a common line, with some deviation at the smallest values of α. This is not unexpected due to the influence of the same quotient on the extensional viscosity (see Fig. 1).

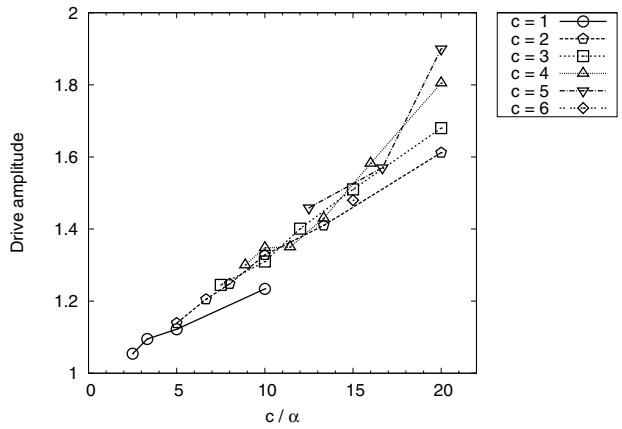

Figure 6. *The amplitude of the drive waveform required to impose a drop speed of U = 6 m/s, plotted against the quotient c/α. Amplitudes are relative to the Newtonian case of pure solvent.*

In Fig. 7 an interpolated heat-map of the drive amplitude over the non-Newtonian parameter space is shown. To give a feel to the numbers, we note that in simulations of Newtonian cases (not shown here) the drive amplitude was found to increase approximately linearly with viscosity, with a value of about 1.5 at 50 mPa s. Diagrams such as Fig. 7 may be useful in practice from an operability perspective, as the known limitations of a printer may impose restrictions on which regions of the parameter space are accessible without compromizing on drop speed.

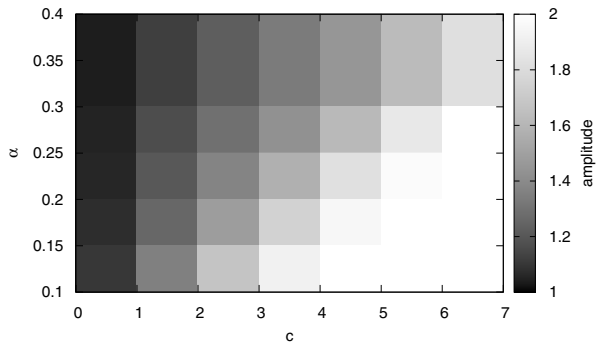

Figure 7. *The drive amplitude as a map over (c, α)-space, with Wi = 2.4.*

The time at which the ligament detaches from the printhead is plotted in Fig. 8 against c/α. In the simulations pinch-off occurs when the ligament develops a neck thinner than 0.5% of the nozzle radius R. There are some crude tendencies: for low c the detachment time increases with α^{-1} while for higher c the opposite occurs, but there is no simple overall trend. Most importantly

however, for all cases considered the time of detachment remains bounded within a fairly narrow interval $\approx$ 50–70 µs, which is a positive aspect of the Giesekus model in comparison to Newtonian cases of high viscosity (50+ mPa s), which have detachment times substantially later than 150 µs, and compared to previous findings for other models of polymer solutions [15] where the pinch-off time may be delayed significantly by viscoelastic effects. Consequently, the ligament length upon detachment is also bounded within a range which compares favourably with other fluid models.

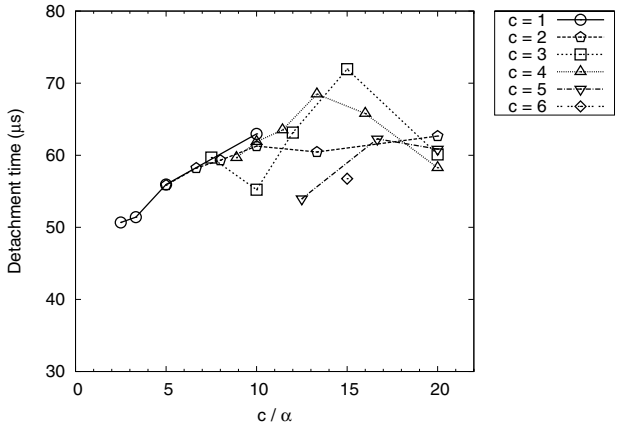

Figure 8. *The time at which detachment of the ligament from the printhead meniscus occurs, plotted against the quotient c/α, with Wi = 2.4.*

To assess the effects of the non-Newtonian parameters on the formation of satellite drops, in keeping with previous work [16] we define the printing 'efficiency' for each case to be the volume proportion of the total ejected fluid which is contained ultimately within the main drop. The efficiency data for our simulations of Giesekus fluids are shown in Fig. 9. The data are plotted against the quantity $c/\sqrt{\alpha}$ because this was found to give the best collapse; however it should be emphasized that the efficiency is an heuristic measure. The overall volume of ink ejected (not plotted here) is roughly proportional to c/α because it is linked directly to the driving amplitude. The efficiency inherits some of this dependence, but is also affected by subtle ligament breakup dynamics.

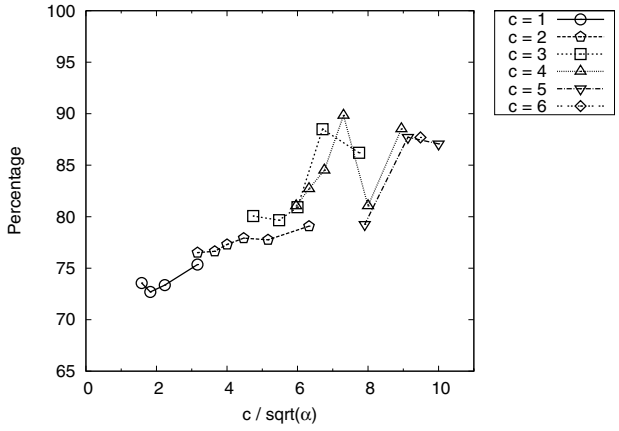

Figure 9. *The printing 'efficiency' (volume proportion of total ejected ink contained within the main drop) plotted against $(c/\sqrt{\alpha})$ with Wi = 2.4.*

The values in Fig. 9 show a quantitative improvement on Newtonian fluids of viscosity up to 15 mPa s (which have efficiency below 75%). In our fixed speed simulations, Newtonian efficiency values approaching 90% may be reached only at much higher viscosities which involve long thin filaments and much later detachment times which are unwieldy for high frequency printing. The efficiency data may also be visualized as a heatmap as shown in Fig. 10 which, together with Fig. 7, represents a 'guide' to the non-Newtonian parameter space in the sense that these diagrams summarize the variation of two of the most critical quantities for performance and operability, respectively.

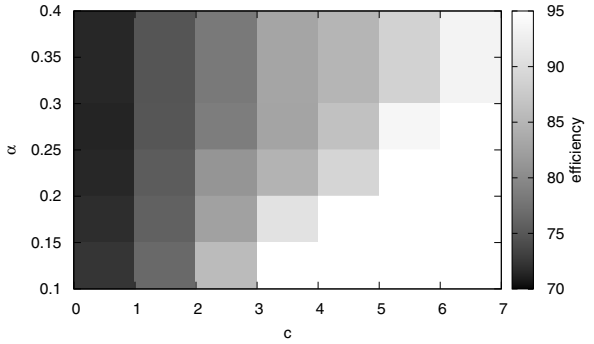

Figure 10. *The variation of 'efficiency' (volume proportion of total ejected ink contained within the main drop) with c and α, for fixed Wi = 2.4.*

It should also be noted that in this study we do not incorporate any collisions or coalescence of drops after ligament breakup has occurred. In some cases it is apparent that such collisions do occur, which, if taken into account, result in small increases to some of the efficiency values as more volume is transferred to the main drop. However, as our aim is to consider non-Newtonian effects on the flow dynamics *prior* to ligament breakup, we choose not to include any coalescence adjustments.

Conclusions and future work

The results shown in these investigations have demonstrated that a combination of viscoelastic and shear-thinning effects could yield improved printing resolution while maintaining a high printing speed and without modifying the drive waveform beyond simple amplification. The proportion of ejected ink contained within the main drop is found to be substantially larger than comparable Newtonian cases, when non-Newtonian parameters are chosen appropriately based on rheological considerations. This improvement is attained without any significant delay in the detachment of the ligament from the printhead.

Further exploration of the parameter space is underway. In particular, the results of varying the relaxation time τ have been omitted here for brevity, as has a detailed study of the transient deformation rate and non-Newtonian stress within the flow. The latter provides important feedback into our understanding and application of the rheology of the Giesekus fluid model, and how our findings differ from those of previous studies where either viscoelastic or shear-thinning effects were considered separately and similar results were established [16]. In addition, by incorporating a variety of solvent viscosities, it should be possible to extend the applicability of these results to other regimes.

Acknowledgments

This work is funded by the U.K. Engineering and Physical Sciences Research Council and the industrial partners in the Innovation in Industrial Inkjet Technology project. The authors thank John Hinch and Gareth McKinley for their helpful comments.

References

[1] O.A. Basaran, H. Gao, and P.P. Bhat, "*Nonstandard inkjets*", Annu. Rev. Fluid Mech., **45** 85 (2013).

[2] B.-J. de Gans, P.C. Duineveld, and U.S. Schubert, "*Inkjet printing of polymers: state of the art and future developments*," Adv. Mater., **16** 203 (2004).

[3] M. Goldin, J. Yerushalmi, R. Pfeffer, and R. Shinnar, "*Breakup of a laminar capillary jet of a viscoelastic fluid*," J. Fluid Mech., **38** 689 (1969).

[4] Y. Christanti and L.M. Walker, "*Effect of fluid relaxation time of dilute polymer solutions on jet breakup due to a forced disturbance*," J. Rheol., **46** 733 (2002).

[5] R.J. Furbank and J.F. Morris, "*An experimental study of particle effects on drop formation*," Phys. Fluids, **16** 1777 (2004).

[6] D.C. Vadillo, A.C. Mulji, and M.R. Mackley, "*The rheological characterization of linear viscoelasticity for ink jet fluids using piezo axial vibrator and torsion resonator rheometers*," J. Rheol., **54** 781 (2010).

[7] R.J. Furbank and J.F. Morris, "*Pendant drop thread dynamics of particle-laden liquids*," Int. J. Multiphase Flow, **33** 448 (2007).

[8] B. Derby, "*Inkjet printing of functional and structural materials: fluid property requirements, feature stability, and resolution*," Annu. Rev. Mater. Res., **40** 395 (2010).

[9] J. Eggers, "*Nonlinear dynamics and breakup of free-surface flows*," Rev. Mod. Phys., **69** 865 (1997).

[10] A.V. Bazilevskiy, J.D. Meyer, and A.N. Rozhkov, "*Dynamics and breakup of pulse microjets of polymeric liquids*," Fluid Dynamics, **40** 376 (2005).

[11] H.J. Shore and G.M. Harrison, "*The effect of added polymers on the formation of drops ejected from a nozzle*," Phys. Fluids, **17** 033104 (2005).

[12] S.D. Hoath, G.D. Martin, J.R. Castrejón-Pita, and I.M. Hutchings, "*Satellite formation in drop-on-demand printing of polymer solutions*," Proc. NIP23, pg. 331 (2007).

[13] D. Xu, V. Sánchez Romaguera, S. Barbosa, W. Travis, J. de Wit, P. Swan, and S.G. Yeates, "*Inkjet printing of polymer solutions and the role of chain entanglement*," J. Mater. Chem., **17** 4902 (2007).

[14] X. Yan, W.W. Carr, and H. Dong, "*Drop-on-demand drop formation of polyethylene oxide solutions*," Phys. Fluids, **23** 107101 (2011).

[15] N.F. Morrison and O.G. Harlen, "*Viscoelasticity in Inkjet Printing*," Rheol. Acta, **49** 619 (2010).

[16] N.F. Morrison and O.G. Harlen, "*Inkjet printing of non-Newtonian fluids*," Proc. NIP27, pg. 360 (2011).

[17] G.H. McKinley, "*Visco-elasto-capillary thinning and breakup of complex fluids*," In Annu. Rheol. Rev. (eds D.M. Binding and K. Walters), British Society of Rheology, **3** 1 (2005).

[18] A.M. Ardekani, V. Sharma, and G.H. McKinley, "*Dynamics of bead formation, filament thinning and breakup in weakly viscoelastic jets*," J. Fluid Mech., **665** 46 (2010).

[19] R. Keunings, "*An algorithm for the simulation of transient viscoelastic flows with free surfaces*," J. Comput. Phys., **62** 199 (1986).

[20] D.W. Bousfield, R. Keunings, G. Marrucci, and M.M. Denn, "*Nonlinear analysis of the surface tension driven breakup of viscoelastic filaments*," J. non-Newtonian Fluid Mech., **21** 79 (1986).

[21] V.M. Entov and E.J. Hinch, "*Effect of a spectrum of relaxation times on the capillary thinning of a filament of elastic liquid*," J. non-Newtonian Fluid Mech., **72** 31 (1997).

[22] M. Renardy, "*Similarity solutions for jet breakup for various models of viscoelastic fluid*," J. non-Newtonian Fluid Mech., **104** 65 (2002).

[23] C. Clasen, J.Eggers, M.A. Fontelos, J. Li, and G.H. McKinley, "*The beads-on-string structure of viscoelastic threads*", J. Fluid Mech., **556** 283 (2006).

[24] O.E. Yildirim and O.A. Basaran, "*Deformation and breakup of stretching bridges of Newtonian and shear-thinning liquids: comparison of one- and two-dimensional models*," Chem. Eng. Sci., **56** 211 (2001).

[25] Z. Gao and K. Ng, "*Temporal analysis of power law liquid jets*," Comput. Fluids, **39** 820 (2010).

[26] P. Doshi, R. Suryo, Ö.E. Yıldırım, G.H. McKinley, and O.A. Basaran, "*Scaling in pinch-off of generalized Newtonian fluids*," J. non-Newtonian Fluid Mech., **113** 1 (2003).

[27] P.J. Carreau, D. De Kee, and M. Daroux, "*An analysis of the viscous behaviour of polymeric solutions*," Can. J. Chem. Eng., **57** 135 (1979).

[28] M. Renardy, "*Self-similar jet breakup for a generalized PTT model*," J. non-Newtonian Fluid Mech., **103** 261 (2002).

[29] M. Renardy and Y. Renardy, "*Similarity solutions for breakup of jets of power law fluids*," J. non-Newtonian Fluid Mech., **122** 303 (2004).

[30] Ö.E. Yıldırım and O.A. Basaran, "*Dynamics of formation and dripping of drops of deformation-rate-thinning and -thickening liquids from capillary tubes*," J. non-Newtonian Fluid Mech., **136** 17 (2006).

[31] M.S. van Deen, T. Bertrand, N. Vu, D. Quéré, E. Clément, and A. Lindner, "*Particles accelerate the detachment of viscous liquids*", Rheol. Acta, **52** 403 (2013).

[32] C. Clasen, P.M. Phillips, L. Palangetić, and J. Vermant, "*Dispensing of rheologically complex fluids: the map of misery*," AIChE Journal, **58** 3242 (2012).

[33] S.D. Hoath, S. Jung, W.-K. Hsiao, and I.M. Hutchings, "*Shear thinning fluids suppress satellite production in high drop speed inkjet printing*", J. non-Newtonian Fluid Mech., IN PRESS (2013).

[34] O.G. Harlen, J.M. Rallison, and P. Szabó, "*A split Lagrangian-Eulerian method for simulating transient viscoelastic flows*," J. non-Newtonian Fluid Mech., **60** 81 (1995).

[35] J.R. Castrejón-Pita, N.F. Morrison, O.G. Harlen, G.D. Martin, and I.M. Hutchings, "*Experiments and Lagrangian simulations on the formation of droplets in drop-on-demand mode*," Phys. Rev. E, **83** 036306 (2011).

[36] H. Giesekus, "*A simple constitutive equation for polymer fluids based on the concept of deformation-dependent tensorial mobility*," J. non-Newtonian Fluid Mech., **11** 69 (1982).

[37] R.B. Bird, R.C. Armstrong, O. Hassager, "*Dynamics of polymeric liquids, Vol. 1, Fluid mechanics*," Wiley, NY, 1987 (2nd ed.).

[38] J. Eggers and E. Villermaux, "*Physics of liquid jets*," Rep. Prog. Phys., **71** 036601 (2008).

[39] W.P. Cox and E.H. Merz, "*Correlation of dynamic and steady flow viscosities*", J. Polym. Sci., **28** 619 (1958).

Author Biography

Neil F. Morrison received his MA in mathematics (2007) and his PhD in complex fluid dynamics (2008) from the University of Cambridge. Since then he has worked at the Department of Applied Mathematics at the University of Leeds. His recent research involves the development of computational techniques for the simulation of flows of complex fluids.

